EVOLUTION & DEVELOPMENT 10:4, 439–448 (2008)

Gene expression reveals unique skeletal patterning in the limb of the direct-developing frog, *Eleutherodactylus coqui*

Ryan Kerney[a,b,*] and James Hanken[a]

[a]Museum of Comparative Zoology, Harvard University, 26 Oxford St., Cambridge, MA 02138 USA
[b]Department of Biology, Dalhousie University, 1355 Oxford St., Halifax, NS, Canada B3H 4J1
[*]Author for correspondence (email: ryankerney@gmail.com)

SUMMARY The growing field of skeletal developmental biology provides new molecular markers for the cellular precursors of cartilage and bone. These markers enable resolution of early features of skeletal development that are otherwise undetectable through conventional staining techniques. This study investigates mRNA distributions of skeletal regulators runx2 and sox9 along with the cartilage-dominant collagen $2_{\alpha}1$ (col2a1) in embryonic limbs of the direct-developing anuran, *Eleutherodactylus coqui*. To date, distributions of these genes in the limb have only been examined in studies of the two primary amniote models, mouse and chicken. In *E. coqui,* expression of transcription factors runx2 and sox9 precedes that of col2a1 by 0.5–1 developmental stage (approximately 12–24 h). Limb buds of *E. coqui* contain unique distal populations of both runx2- and sox9-expressing cells, which appear before formation of the primary limb axis and do not express col2a1. The subsequent distribution of col2a1 reveals a primary limb axis similar to that described for *Xenopus laevis*. Precocious expression of both runx2 and sox9 in the distal limb bud represents a departure from the conserved pattern of proximodistal formation of the limb skeleton that is central to prevailing models of vertebrate limb morphogenesis. Additionally, runx2 is expressed in the early joint capsule perichondria of the autopod and in the perichondria of long bones well before periosteum formation. The respective distributions of sox9 and col2a1 do not reveal the joint perichondria but instead are expressed in the fibrocartilage that fills each presumptive joint capsule. These distinct patterns of runx2- and sox9-expressing cells reveal precursors of chondrocyte and osteoblast lineages well before the appearance of mature cartilage and bone.

INTRODUCTION

The life history of most frog species is biphasic; an aquatic tadpole metamorphoses into a terrestrial adult. Many species, however, exhibit variations on this common theme. The most dramatic departure from biphasic development is direct development, which in the neotropical frog *Eleutherodactylus coqui* is characterized by the deposition of terrestrial eggs that hatch as miniature froglets instead of aquatic tadpoles (Orton 1951; Hanken 2003; Sampson 1900; Elinson 2001). Whereas limb bud formation in metamorphosing anurans typically begins during the tadpole stage, well after embryogenesis, limb formation in *E. coqui* begins in the embryo before complete closure of the neural tube (Elinson 1994; Richardson et al. 1998). In the clawed frog *Xenopus laevis*, a metamorphosing species, the hind limb bud is first apparent in the tadpole by approximately 7.5 days (stage 48; Nieuwkoop and Faber 1994) and limb chondrogenesis proceeds over the next 5 weeks (Trueb and Hanken 1992; Nieuwkoop and Faber 1994). In *E. coqui*, the hind limb bud is first apparent in the 4-day embryo (stage 3; Townsend and Stewart 1985) and limb chondrogenesis proceeds over just 10 days (Townsend and Stewart 1985; Hanken et al. 2001). Early limb development in direct-developing *E. coqui* is convergent with the embryonic limb development of amniotes. However, the extent to which this convergence of developmental timing coincides with other developmental features is largely unknown.

One unique feature of limb development in *E. coqui* among anurans is the lack of a morphologically distinct apical ectodermal ridge (AER; Richardson et al. 1998; Hanken et al. 2001), a signaling center that is generally regarded as essential for establishing the proximodistal axis of the developing limb (Saunders 1948). The AER is present in all metamorphosing frogs that have been examined (Hanken 1986). Studies of *Xenopus laevis* reveal a distinct AER (Tarin and Sturdee 1971, 1974) and active signaling from the AER region (Tschumi 1957), which coincides with the conserved expression of Fgf-8 (Christen and Slack 1997). Absence of an AER in *E. coqui* is convergent with salamanders, the only other tetrapod group known to lack this anatomical structure (Hanken 1986). Absence of an AER in salamanders is correlated with the early formation of distal skeletal elements in the limb before the

© 2008 The Author(s)
Journal compilation © 2008 Blackwell Publishing Ltd.

appearance of more proximal skeletal condensations (Shubin and Alberch 1986; Wake and Shubin 1998; Shubin and Wake 2003; Franssen et al. 2005). The pattern of Alcian blue-positive cartilage formation in *E. coqui* does not reveal early distal skeletal elements such as those found in salamanders (Hanken et al. 2001), but limb development in this species has not been examined using earlier markers of skeletal differentiation. These markers might reveal patterning that is not detectable through conventional techniques (sensu Welten et al. 2005; Kerney et al. 2007a).

Development of the vertebrate limb skeleton typically follows a conserved pattern of proximal-to-distal differentiation (Holmgren 1933; Hinchliffe and Johnson 1980; Hinchliffe and Griffiths 1982; Burke and Alberch 1985; Shubin and Alberch 1986). This proximodistal order is detectable with markers at several levels of skeletal differentiation, including extracellular matrix staining with alizarin red and Alcian blue (e.g., Hanken et al. 2001) and analyses of mesenchymal condensations that prefigure skeletal elements (e.g., Shubin and Alberch 1986). Developmentally early markers of cartilage-forming cells (chondrocytes), including immunoreactivity with the type II collagen antibody (Linsenmayer and Hendrix 1980) and expression of the type II collagen precursor gene col2a1, also reveal conserved proximodistal patterning of the limb skeleton (Swalla et al. 1988; Nakamura et al. 2006; Chen et al. 2007). The transcription factors sox9 and runx2 are both expressed in limb skeleton where they are required for the differentiation of chondrocytes and osteoblasts, respectively (Wright et al. 1995; Ducy et al. 1997; Komori et al. 1997; Otto et al. 1997). These genes are among the earliest markers of the prospective skeleton and their distribution reveals the earliest patterning of skeletal precursors (reviewed in Hall 2005). Both sox9 (Chimal-Monroy et al. 2003; Welten et al. 2005) and runx2 (Kim et al. 1999) are expressed in the conserved proximodistal order found in later skeletal markers of cartilage and bone. To date, however, the distribution of these transcription factors has only been analyzed in limbs of the two prevailing amniote models, mouse and chicken.

The present study investigates early patterning of the limb skeleton in *E. coqui* through the expression of the transcription factors runx2 and sox9 and the cartilage-dominant collagen, col2a1. Expression of these genes represents a key link between the initial patterning events of the limb and the formation of skeletal condensations along the proximodistal axis. Their distribution may reveal any alterations in proximodistal patterning of the limb skeleton that coincide with the absence of a morphologically distinct AER in *E. coqui*. This information, in turn, provides the first detailed analysis of chondrocyte and osteoblast precursors in amphibian limbs and contributes to our understanding of developmental novelties of *E. coqui* limb development and current models of proximodistal patterning within the vertebrate limb skeleton.

MATERIALS AND METHODS

E. coqui collection and breeding

Thirty adult *E. coqui* were collected from the Caribbean National Forest near El Verde, Puerto Rico, under permits from the Departamento de Recursos Naturales y Ambientales (DRNA 03-IC-067). The frogs were returned to a breeding colony in Cambridge, MA, where they were housed in breeding pairs or triplets in glass aquaria, sprayed daily and fed crickets supplemented with Repta Calcium Supplement (Fluker Farms; Port Allen, LA). After 3 months in captivity the females began producing clutches of eggs. These were either left with the male or removed and incubated in a Petri dish at 25°C. Breeding and maintenance of embryos followed standard protocols (Hanken et al. 2001), which were approved by the Harvard University/Faculty of Arts and Sciences Standing Committee on the use of Animals in Research and Teaching (protocol 99-09). An Animal Welfare Assurance statement is on file with the university's Office for Laboratory Welfare (OLAW).

Cloning of runx2, sox9 and col2a1

Portions of the runx2, sox9 and col2a1 genes were amplified from *E. coqui* cDNA through PCR. Total RNA was extracted from bone (runx2) or whole embryos (sox9 and col2a1) with Trizol (Invitrogen; Carlsbad, CA) following the manufacturer's protocol. cDNA was synthesized with the Superscript II Reverse Transcription kit (Invitrogen). The runx2 primers used were 5′-TCACGATA ACCGGACAATGG-3′ (forward) and 5′-GATTCATCCATTC GACCACT-3′ (reverse), which produced a 1207 base pair (bp) product (Genbank accession no. EF428557). The sox9 primers used were 5′-GASAARTTCCCCGTGTGCATC-3′ (forward) and 5′-YARGGYCTTGTGAGCTGTGTGTA-3′ (reverse), which amplified an 1181 bp product (Genbank accession no. EF428559). A smaller, 538-bp region of sox9 was re-cloned for use as an in situ hybridization probe with 5′-AGAGGATGGTTCTGAGCA GACCC-3′ (forward) and 5′-TGAGGTGGCTGTTGCTGTTTG G-3′ (reverse) primers. A nested PCR was used to amplify col2a1. Outside primers were 5′-ACATGCCKGCHGAYSARGC-3′ (forward) and 5′-CCWCCRATRTCCATDGGWAGCRATGTC-3′ (reverse), which produced a smear on the gel at a lower annealing temperature (55°C). Inside primers were 5′-GARAARGGMCCCG AYCCYCTG-3′ (forward) and 5′-GCCTTCTTSAGGTTGCC WG-3′ (reverse), which produced a final, 528-bp product (Genbank accession no. EF428558). These PCR products were ligated into the pcrII vector and cloned with One Shot cells with the TOPO TA cloning kit (Invitrogen).

Phylogenetic analysis

Both maximum parsimony and Bayesian analyses of the protein sequences from Runx, SoxE and fibrillar-collagen vertebrate gene families were performed to establish orthology of the genes cloned from *E. coqui*. Descriptions of the analyses, consensus phylogenies and comparisons with former gene trees are included in online supporting material (Appendix S1).

Whole mount in situ hybridizations

Whole mount in situ hybridizations were performed on 44 embryos, TS stages 5–10 (Townsend and Stewart 1985; Table 1),

Table 1. Number of whole-mount in situ hybridizations for each gene over seven developmental stages

TS Stage	Col2al	Sox9	Runx2
5	3	2	6
6	2	1	2
7	2	2	1
7.5	3	2	2
8	1	3	1
9	2	2	3
10	1	2	1

Staging follows Townsend and Stewart (1985; TS) except for stage 7, which is divided into two parts. Stage 7.5 is further described in the text.

following standard *Xenopus* protocols (Sive et al. 2000) modified for the larger *Eleutherodactylus* embryos. Before fixation, younger embryos (TS 5–6) were treated with a 0.5% cysteine solution (pH 8.5) for 10 min followed by several washes in phosphate-buffered saline. This loosened the outer fertilization membrane and facilitated removal of the embryo with watchmaker forceps. Antisense RNA was created with a Maxiscript Sp6 in vitro transcription kit (Ambion; Austin, TX) on linearized templates. A mixture of 33% digoxygenin-labeled UTP (Roche; Basel, Switzerland) to 66% unlabeled UTP was used in the transcription reaction. Embryos were fixed in MEMFA for 2 h at room temperature and stored in 70% ethanol at -20°C. The proteinase K treatment step was increased to 10 min at room temperature to accommodate the larger embryos. All hybridizations were carried out overnight at 55°C. Stained embryos were stored in 70% methanol at 4°C.

RESULTS

Stage 5

Runx2 is the only gene expressed in the limb during stage 5. It is seen in the distal mesenchyme of both fore- and hind limbs (Figs. 1 and 2).

Stage 6

Runx2 expression continues in the distal mesenchyme of fore- and hind-limb buds early in stage 6. Hind-limb expression includes distinct regions that correspond to the presumptive femur, tibia and fibula. Later in stage 6, runx2 expression expands to the more distal fibulare (calcaneum) and tibiale (astragalus—although see Blanco et al. 1998 for alternate homologies; Fig. 2).

Sox9 is not expressed in the forelimb during stage 6. Its initial expression in the hind limb appears in a proximal region that corresponds to the approximate location of the future femur, tibia and fibula, and in a single distal region of mesenchyme that corresponds to the axial digit (digit IV; Fig. 2).

Col2a1 also is not expressed in the forelimb during stage 6. It is co-expressed with sox9 in the proximal portion of the hind limb, revealing a well-defined femur and less distinct tibia and fibula. Col2a1 does not evince the distal mesenchymal expression seen in both sox9- and runx2-stained limbs at this stage (Fig. 2).

Stage 7

Runx2 expression in the limbs expands dramatically. Initial expression in the forelimb continues in the distal mesenchyme, with the addition of a region of proximal expression that corresponds to the future humerus (Fig. 1). By stage 7.5 the proximal expression includes the future radius and ulna, whereas the distal mesenchymal expression is divided into two regions that correspond to digits III and IV.

Distal hind limb expression of runx2 divides into digits IV and V early in stage 7 (Fig. 2). There is also faint expression in the presumptive tibiale and fibulare, which become more distinct later in the stage. Runx2 expression includes digit III by stage 7.5, when metatarsal IV begins to show the formation of the first metatarsal–phalangeal joint. The condensation of digit IV is continuous with the distal perichondrium that surrounds the metatarsal–phalangeal joint (Joyce and Cohen 1970). Perichondrial staining eventually occurs in metacarpal–phalangeal and interphalangeal joints of the manus, but never appears in elbow, knee, wrist or ankle joints.

Runx2 expression ultimately becomes restricted to the perichondrium in the stylopod and zeugopod of both fore- and hind limbs. The gene is expressed initially through the center of these presumptive skeletal elements (Fig. 1B), but by stage 7.5 expression is restricted to the perichondrium of the diaphysis. Expression becomes confined to the perichondrium of successively distal skeletal elements during subsequent stages (data not shown).

Sox9 expression begins in the forelimb during stage 7. The gene is expressed initially in the humerus, radius and ulna (Fig. 1), but there is a separate distal region of expression in the precursor of digit III, which resembles the axial expression seen in digit IV of the pes during stage 6. Branching of the radius and ulna becomes distinct by stage 7.5, along with additional expression in digits II and IV. In the hind limb, initially separate regions of sox9 expression in the presumptive fibula and digit IV become continuous early in stage 7 (Fig. 2). There also is a region of expression anterior to the base of digit IV, which corresponds to the tarsal arch. Sox9 expression in individual skeletal elements becomes more distinct by stage 7.5. The fibulare and tibiale begin to divide from the tibia and fibula, and there is additional expression in digits III and V. Sox9 expression in digit IV encompasses runx2 staining on stage-matched limbs, but does not reveal the perichondral joint capsule evident in runx2-stained digits.

Col2a1 expression in the forelimb begins in the humerus, along with an indistinct branching of the radius and ulna (Fig. 1). Unlike both sox9 and runx2, which show additional,

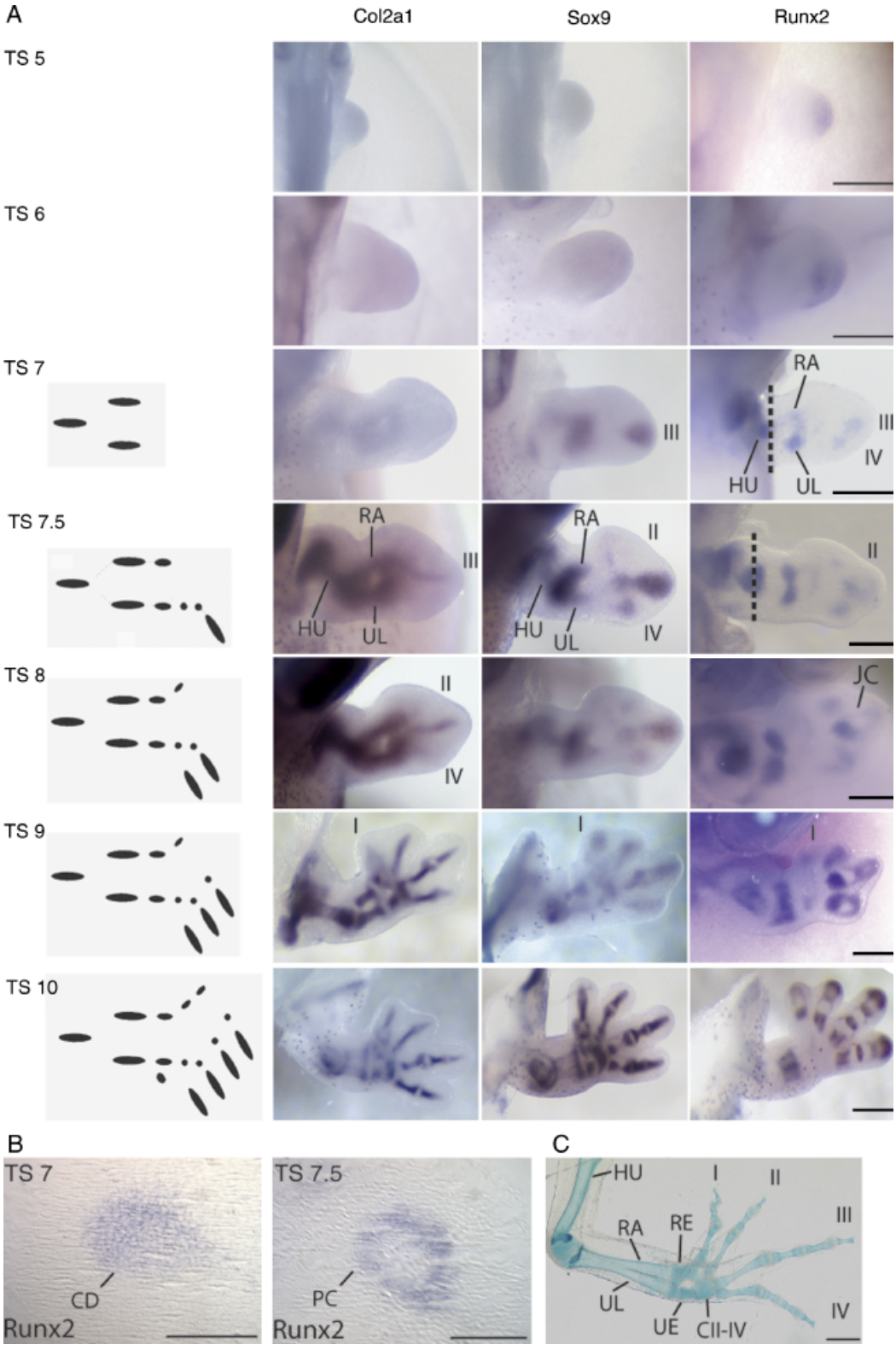
A
Col2a1
Sox9
Runx2
TS 5
TS 6
TS 7
TS 7.5
TS 8
TS 9
TS 10
RA
HU
UL
III
II
IV
I
JC
B
TS 7
CD
Runx2
TS 7.5
PC
Runx2
C
HU
I
II
III
RA
RE
UL
UE
CII-IV
IV

early regions of distal expression, col2a1 is confined initially to proximal elements. Subsequently, col2a1 expression expands distally; by stage 7.5 the radius and ulna are clearly divided and there is continuous staining through digit III. In the hind limb, col2a1 expression is distinct in the presumptive femur, tibia and fibula early in stage 7 (Fig. 2). By stage 7.5 this expression expands to include the fibulare, tarsal arch and digit IV. Col2a1 staining in digit III of the forelimb and digit IV of the hind limb is narrow at stage 7.5 compared with the distribution of sox9. Neither sox9 nor col2a1 is expressed in the perichondrium of the first metacarpal–phalangeal joints, which express runx2.

Stage 8

Limb cartilages begin to stain with Alcian blue (Hanken et al. 2001). These include the femur/humerus (stylopodium), radius/tibia and ulna/fibula (zeugopodium), tibiale, fibulare, metacarpal III and metatarsals II–V. This distribution of Alcian blue staining corresponds to the distribution of col2a1 mRNA at the same stage. Unlike the early expression of runx2 and sox9, however, there are no separate distal regions of Alcian staining in the limb.

Runx2 expression incorporates additional digits in a posterior to anterior order. In the forelimb, digit III shows increased staining in the metacarpal–phalangeal joint and there is expanded expression in digits II and IV (Fig. 1). In the hind limb, the perichondrium of the metatarsal–phalangeal joint is runx2 positive in digits IV and V (Fig. 2). Digit IV shows additional staining in the second phalanx and around its joint with the third phalanx.

Sox9 remains confined to presumptive skeletal elements. In the forelimb, its expression in digits II and IV expands distally (Fig. 1). In the hind limb, it is expressed in distinct precursors of the tibiale and fibulare along with digits III–V (Fig. 2). The expression domain of sox9 around the metatarsal–phalangeal joint is thickened, although it still does not show the clear division of the joint, which is revealed in runx2-stained limbs.

Col2a1 also expands to additional digits. In the forelimb, it is expressed in a narrow band along digit III with faint additional staining in digits II and IV (Fig. 1). The hind limb similarly has additional narrow lines of staining in digits III and V along with more distinct staining of the fibulare (Fig. 2). There is diffuse staining around the tibiale throughout stage 8. Although expression of col2a1 resembles the distribution of Alcian blue during this stage (Hanken et al. 2001), Alcian staining is restricted to the center of each cartilage while the expression of col2a1 is continuous between the individual skeletal elements. There are some regions of weak col2a1 staining in the prospective joints, but col2a1 expression is not restricted from the joint cavities until later stages.

Stage 9

Runx2 expression in the phalanges expands in proximodistal order. Additional perichondria of the interphalangeal joints, revealed by runx2 staining, are added before the next distal phalanx forms. Expression in the forelimb includes all four digits, although joints are not yet visible in digits I and II (Fig. 1). Expression in the hind limb includes all five digits, with digits I and II appearing faint and unjointed (Fig. 2).

Sox9 is expressed in all five digits of the hind limb and four digits of the forelimb. In the forelimb, there is distinct staining in the future radiale, ulnare and fused carpals II–IV; other elements of the wrist are not yet distinct (Fig. 1). In the hind limb, sox9 expression is restricted to epiphyses of the femur, tibia and fibula, whereas expression in the tibiale and fibulare is continuous along the entire length of the condensation (Fig. 2). Thickened staining in digits IV and V corresponds to the future metatarsal–phalangeal joint, which is apparent by stage 7 in runx2-stained hind limbs. Col2a1 expression is well defined in most skeletal elements of the fore- and hind limbs. Expression in the humerus, femur, tibia and fibula is largely restricted to the epiphyses. In the forelimb, col2a1 is expressed in all four digits, with clear differentiation of digits II–IV and diffuse expression in digit I (Fig. 1). The metacarpal–phalangeal joint is apparent in digit III and is beginning to appear in digit IV. There also is clear definition of the ulnare, radiale and carpals II–IV. In the hind limb, there is distinct staining in digits II–V, with initial segmentation in digits III–V and the first metatarsal-phalangeal joint in digits IV–V (Fig. 2). There is faint expression in the region of digit I. As seen during stage 8, the distribution of col2a1 during stage 9 closely resembles the distribution of Alcian blue (Hanken

Fig. 1. Distribution of col2a1, sox9 and runx2 transcripts in the developing forelimb. (A) Dorsal views of right limbs. The left column is modified from Shubin and Alberch's (1986) model of forelimb condensation formation in *Xenopus laevis*. The other columns show the distribution of col2a1, sox9 and runx2 over several Townsend and Stewart (1985; TS) embryonic stages. The Shubin and Alberch model is realized only in the expression of col2a1. Sox9 and runx2 instead are expressed initially in distal domains, which are separate from the proximal condensations by stage 7. Early joint formation in the manus is apparent with runx2 by stage 8. mRNA is expressed around the perichondrium of each successive joint capsule (JC) and precedes the joint divisions revealed by sox9 or col2a1 staining by one developmental stage. Images in each row are depicted at the same scale; scale bar, 0.25 mm. (B) Transverse sections of runx2-stained forelimbs. Planes of section are depicted by the dashed lines through the humerus (HU) in the corresponding panels in A. Runx2 initially is expressed throughout the skeletal condensation (TS 7, CD), but later it is restricted to the future perichondrium (TS 7.5, PC). Scale bars, 0.125 mm. (C) Dorsal view of Alcian blue-stained forelimb, stage 15. Radius (RA) and ulna (UL) have fused. The prepollex lies ventral to the first digit and is not visible here. Scale bar, 0.25 mm. Additional abbreviations: CII–IV, fused carpals II through IV; RE, radiale; UE, ulnare. Digits are identified with Roman numerals I–IV.

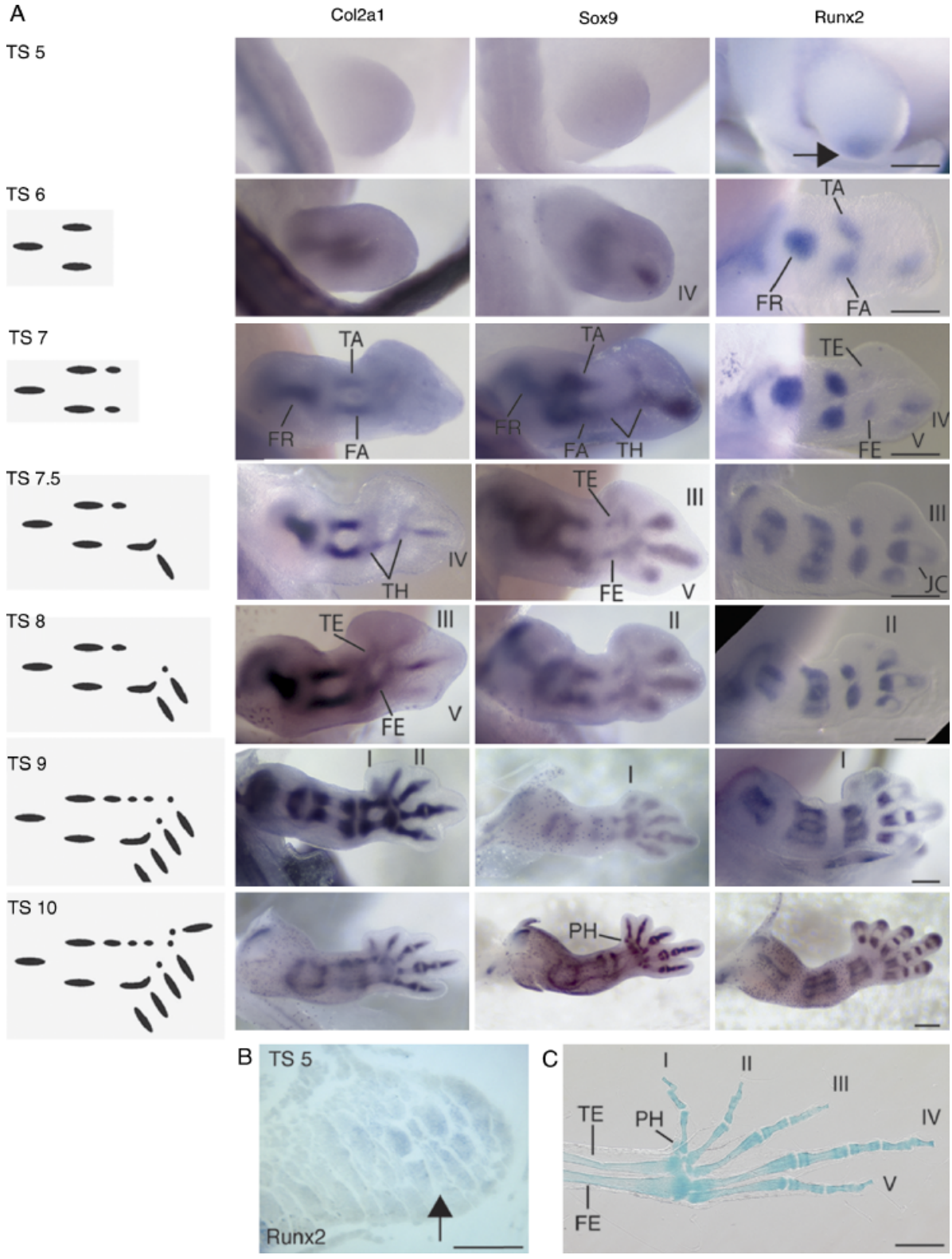
A
Col2a1
Sox9
Runx2
TS 5
TS 6
TS 7
TS 7.5
TS 8
TS 9
TS 10
TA
FR
FA
IV
TH
TE
III
FE
V
II
I
PH
JC
B
TS 5
Runx2
C
I
II
III
IV
V
TE
PH
FE

et al. 2001), although the diffuse expression of col2a1 in digit I of each limb is not apparent in Alcian blue staining.

Stage 10

Runx2 reveals the future bony skeleton, with conspicuous exception of the tarsals, carpals, radiale and ulnare, which do not express the gene in any of the stages examined here. Its expression depicts phalangeal formulae of 1-2-3-3 in the forelimb (Fig. 1) and 1-2-3-4-3 in the hind limb (Fig. 2). These approach the adult formulae of 2-2-3-3 and 2-2-3-4-3, respectively. Distal-most phalanges are rounded, with strong expression extending to the end of each finger and toe. Runx2 expression is restricted to the perichondrium of all skeletal diaphyses in both limbs.

Sox9 becomes restricted to limb-skeletal epiphyses in a proximal-to-distal direction. The transcript is expressed primarily in epiphyses of proximal long bones, metacarpals III–IV and metatarsals IV–V. Fewer phalanges are revealed by sox9 staining than by runx2, yielding somewhat reduced phalangeal formulae of 1-1-2-2 (forelimb; Fig. 1) and 1-1-2-3-2 (hind limb; Fig. 2). Sox9 is not expressed in distal-most phalanges, which are clearly stained by runx2. However, sox9 staining does reveal the ulnare, radiale, prepollex and fused carpals II–IV in the forelimb, none of which expresses runx2 at any stage examined.

Col2a1 mRNA is concentrated primarily in epiphyses of proximal long bones; it reveals fewer phalanges in the autopod than sox9 or runx2. Each digit is well defined, with phalangeal formulae of 0-1-2-1 (forelimb; Fig. 1) and 0-0-1-2-1 (hind limb; Fig. 2). As with sox9, radiale, ulnare and fused carpals are distinct with col2a1, whereas the prepollex is not stained in any hind limb analyzed (Fig. 1).

DISCUSSION

Direct development in the genus *Eleutherodactylus* represents the most extreme departure from the ancestral biphasic life history of any anuran examined to date (Orton 1951; Elinson et al. 1990; Kerney et al. 2007b). Coincident with this change in life history is dramatic acceleration of limb development from the metamorphic to the embryonic stage of development. While embryonic formation of the limb is thus convergent with amniote development, the early limb of *E. coqui* has several unique features not found in amniotes. These include lack of the AER (Richardson et al. 1998; Hanken et al. 2001), a relatively earlier offset of signaling from the zone of polarizing activity (Hanken et al. 2001), and a unique differentiation of distal skeletal precursors before more proximal elements arise (this article). Limb-skeletal patterning in *E. coqui*, as revealed through expression of runx2, sox9 and col2a1, bears on several prevailing models of limb skeletal development and evolution in vertebrates.

Proximodistal patterning of the limb

Formation of skeletal condensations in the limb follows a strict proximodistal sequence in all tetrapods except salamanders. Whereas expression of runx2, sox9 and col2a1 mirrors this conserved proximodistal order in amniotes (Kim et al. 1999; Akiyama et al. 2005; Nakamura et al. 2006), runx2 and sox9 each show unique distal expression in *E. coqui*, which appears before the formation of more proximal elements. This distal expression is unexpected given the conserved proximodistal order of both col2a1 mRNA expression (Figs. 1, A and 2A) and the type-II collagen protein product (Kerney and Hanken, unpublished observation), as well as the proximodistal deposition of proteoglycans revealed by Alcian blue staining (Hanken et al. 2001). Initially, a wide domain of runx2 is expressed in the early limb bud, which corresponds topographically to the autopodial expression of runx2 in later stages. Sox9 is expressed in the axial digit of the fore- and hind limb buds in a discrete domain that is distal to its initial expression in the stylopod and zeugopod. At present, the expression of neither gene has been described for the limbs of any tetrapods except chickens, mice and *E. coqui*. This lack of comparative data makes it impossible to determine whether these distal expression domains are unique to *E. coqui* or are a more general feature of anuran—or possibly amphibian—development.

Shubin and Alberch (1986) proposed a morphogenetic model of limb patterning based on the formation of skeletal condensations along a primary axis of the limb skeleton. This axis runs from the humerus/femur through the ulna/fibula, along a carpal/tarsal arch, and through the metacarpal of a single axial digit (Figs. 1 and 2). In anurans, the axial digit first appears as metacarpal III in the four-fingered forelimb and as metacarpal IV in the five-toed hind limb (Shubin and Alberch 1986). According to their model, differential branching and segmentation of these condensations account for eventual patterning of the limb skeleton in a proximodistal order. The expression of sox9 and runx2 in *E. coqui* reveals a different pattern of skeletal precursor differentiation along the

Fig. 2. Distribution of col2a1, sox9 and runx2 transcripts in the developing hind limb. (A) Dorsal views of right limbs. The left column is modified from Shubin and Alberch's (1986) model of hind limb condensation formation in *Xenopus laevis*. Expression of col2a1 follows the model, whereas both sox9 and runx2 are expressed early in separate proximal and distal regions. As in the forelimb, early patterning of the joint capsule (JC) is apparent in runx2 expression before any subdivision of col2a1 or sox9 digital staining. (B) Coronal section of a stage-5 hind limb stained with the anti-runx2 probe. Mesenchymal expression first appears distally (arrow). (C) Dorsal view of Alcian blue-stained foot, stage 15. The prehallux (PH) is visible anterior to the first digit. Scale bars, 0.25 mm. Additional abbreviations: FA, fibula; FE, fibulare; FR, femur; TA, tibia; TE, tibiale; TH, tarsal arch. Digits are identified with Roman numerals I–V.

primary axis of the limb, wherein distal elements differentiate before proximal ones. Whereas the distribution of skeletal condensations revealed by col2a1 staining does constitute the primary axis of the limb (Figs. 1 and 2), the establishment of this axis results from the connection of proximal and distal domains of sox9- and runx2-expressing precursors. Early development of these precursors does not follow the morphogenetic rules posited by the Shubin and Alberch (1986) model, and instead suggests an initial patterning of the limb skeleton that is not identifiable through the analysis of condensations or other conventional markers of skeletal differentiation.

The exact role of the AER in establishing proximodistal limb patterning in amniotes is unresolved. Contrasting models differ with respect to the relative timing of specification versus differentiation of the early limb skeleton. The initial "progress zone" model describes a progressive proximodistal specification that is dependent on the amount of time precursor cells spend in the mesenchyme subjacent to the AER (Summerbell et al. 1973). In this model, specification roughly coincides with differentiation, which occurs once precursors are released from AER signaling (Niswander et al. 1994; Mahmood et al. 1995). The more recent "early specification model" describes a different function for AER signaling in preventing cell death in the "progress zone" region (Dudley et al. 2002; Sun et al. 2002). This model describes an early specification of each skeletal element in the early limb bud, with subsequent proximodistal differentiation of these elements during outgrowth. A third alternative is based on early patterns of segmental gene expression inside the limb, where a proposed "undifferentiated zone" is maintained subjacent to the AER; segments are specified through a combination of proximal and distal signals (Mercader et al. 2000; Tabin and Wolpert 2007). In *E. coqui*, early distal expression of runx2 and sox9 does not appear to be consistent with any of these amniote-based models. None, for example, predicts early distal differentiation of skeletal precursors before more proximal elements, and neither sox9 nor runx2 exhibits early distal expression in amniotes (Kim et al. 1999; Akiyama et al. 2005). Early distal expression of sox9 and runx2 in *E. coqui* may indicate an alternate, and unknown, mechanism of limb patterning in these and perhaps other direct-developing amphibians.

Unique expression of Runx2

In the developing mouse limb, early, widespread expression of sox9 eventually becomes restricted to differentiated chondrocytes (Chimal-Monroy et al. 2003). All runx2-expressing cells descend from sox9-expressing precursors (Akiyama et al. 2005). This sequence of gene expression is reversed in limb buds of *E. coqui*: early expression of runx2 in distal fore- and hind limb buds precedes, rather than follows, expression of sox9. Thus, in *E. coqui* runx2-expressing cells are not descendents of a sox9-expressing lineage. Whereas this surprising result could indicate a non-skeletogenic fate of distal runx2-expressing cells in *E. coqui*, these cells correspond topographically to autopodial phalanges of the axial and post-axial digits in our developmental series (Figs. 1 and 2), which strongly suggests that they are skeletogenic precursors.

Stylopod, zeugopod and autopod differences

Runx2 is expressed initially through the center of each stylopod and zeugopod diaphysis. However, by stage 7.5 the gene is expressed exclusively in the perichondrium of these diaphyses (Fig. 1B). In mice, perichondrially expressed Runx2 inhibits chondrocyte maturation in the growth plate through positive regulation of Fgf18 signaling (Hinoi et al. 2006). This role may be conserved in *Eleutherodactylus coqui*, or the perichondrial runx2 expression may simply mark precursors of the periosteum. Sox9 and col2a1 are initially expressed more broadly along the entire limb axis. Eventually, expression of both sox9 and col2a1 is restricted to epiphyses of long bones in regions corresponding to cartilaginous growth plates. By stage 10, epiphyseal expression of sox9 and col2a1 barely overlaps the diaphyseal expression of runx2 in the perichondria. These distinct patterns of runx2 and sox9 expression coincide with the expected osteoblast and chondrocyte lineages of the early limb skeleton, respectively.

Expression of runx2 differs from both sox9 and col2a1 in its early definition of autopodial joint capsules. In anurans, these capsules are differentiated in a proximodistal order with the initial formation of a perichondrial sheath around the presumptive joint (Joyce and Cohen 1970). Runx2 staining around the joint capsule delineates this perichondrium, whereas both sox9 and col2a1 are expressed throughout the entire presumptive joint cavity in the early digit. Their expression corresponds with the fibrocartilage that fills the joint capsule early in development (Joyce and Cohen 1970). However, joint capsule fibrocartilage does not express runx2. Neither sox9 nor col2a1 is expressed in the later joint capsule, corresponding to the expected degradation of the joint capsule fibrocartilage (Joyce and Cohen 1970).

Whereas both sox9 and col2a1 reveal mesopodial (carpal and tarsal) elements, runx2 is not expressed in any of these structures during the stages examined. This lack of runx2 expression is unexpected given its typical distribution in cartilages fated to be replaced by bone (Eames et al. 2004). Runx2 may be expressed in these elements after TS10, as anuran carpals and tarsals typically ossify after the rest of the limb (Trueb and Hanken 1992), or runx2 expression may not be detectable through the whole-mount methods used in this study. The tibiale and fibulare of anurans are typically regarded as mesopodial elements, homologous to the astragalus and calcaneum of amniotes (Duellman and Trueb 1994). Yet, zeugopodial origin of the tibiale and fibulare has been sug-

gested due to the expanded expression of Hoxa-11 in the anuran hindlimb bud (Blanco et al. 1998). Early expression of runx2 in the tibiale and fibulare, and its apparent absence from all tarsal precursors, further supports the proposed zeugopodial origin of these bones. Alternatively, expression of runx2 in the tibiale and fibulare may simply reflect their early ossification when compared with other carpal and tarsal elements.

CONCLUSIONS

The spatial distribution and timing of gene expression associated with chondrocyte and osteoblast differentiation reveals important aspects of limb-skeletal patterning that are not obtainable with conventional techniques. The direct-developing frog *Eleutherodactylus coqui* shows unexpected early distal formation of skeletogenic precursors that is not seen in amniotes. Expression of the genes runx2 and sox9 differs among limb segments. In the stylopod and zeugopod, distribution of runx2 and sox9 reveals a separation of chondrocyte and osteoblast cell lineages. In the autopod, runx2 is expressed in each phallanx and in the perichondria of each joint capsule, whereas sox9 and col2a1 are expressed in the phalanges and through the center of each capsule. Dynamic expression of these genes in the limb of *E. coqui* reveals both conservation with and differences from amniote development, and further illustrates the value of comparative studies in revealing diverse developmental pathways that may go undetected by analysis of a limited array of model systems. It would be especially interesting to assess patterns of gene expression during limb development in salamanders. Like *E. coqui*, these vertebrates lack a morphologically discrete AER but, unlike all other tetrapods, they also show early formation of distal limb skeletal elements.

Acknowledgments

The authors thank José Rosado for assistance in collecting *E. coqui* in Puerto Rico and Anne Everly for her attentive animal care in Cambridge. Bjorn Olsen and members of his lab gave excellent advice and direction during the cloning of runx2. Josh Gross and two anonymous reviewers commented on previous versions of this manuscript. Financial support was provided by a Goelet Research Grant from the Museum of Comparative Zoology (RK) and NSF grant EF-0334846 (AmphibiaTree; JH).

REFERENCES

Akiyama, H., et al. 2005. Osteo-chondroprogenitor cells are derived from Sox9 expressing precursors. *Proc. Natl. Acad. Sci. USA* 102: 14665–14670.

Blanco, M. J., Misof, B. Y., and Wagner, G. P. 1998. Heterochronic differences of hoxa-11 expression in *Xenopus* fore- and hind limb development: evidence for lower limb identity of the anuran ankle bones. *Dev. Genes Evol.* 208: 175–187.

Burke, A., and Alberch, P. 1985. The development and homology of the chelonian carpus. *J. Morphol.* 186: 119–131.

Chen, M., et al. 2007. Generation of a transgenic mouse model with chondrocyte-specific and tamoxifen-inducible expression of Cre recombinase. *Genesis* 45: 44–50.

Chimal-Monroy, J., et al. 2003. Analysis of the molecular cascade responsible for mesodermal limb chondrogenesis: Sox genes and BMP signaling. *Dev. Biol.* 257: 292–301.

Christen, B., and Slack, J. M. 1997. FGF-8 is associated with anteroposterior patterning and limb regeneration in *Xenopus*. *Dev. Biol.* 192: 455–466.

Ducy, P., Zhang, R., Geoffry, V., Ridall, A. L., and Karsenty, G. 1997. Osf2/CBFa1: a transcriptional activator of osteoblast differentiation. *Cell* 89: 747–754.

Dudley, A. T., Ros, M. A., and Tabin, C. J. 2002. A re-examination of proximodistal patterning during vertebrate limb development. *Nature* 418: 539–544.

Duellman, W. E., and Trueb, L. 1994. *The Biology of Amphibians*. Johns Hopkins University Press, Baltimore, MD.

Eames, F. B., Sharpe, P. T., and Helms, J. A. 2004. Hierarchy revealed in the specification of three skeletal fates by *Sox9* and *Runx2*. *Dev. Biol.* 274: 188–200.

Elinson, R. 1994. Leg development in a frog without a tadpole (*Eleutherodactylus coqui*). *J. Exp. Zool.* 270: 202–210.

Elinson, R. 2001. Direct development: an alternative way to make a frog. *Genesis* 29: 91–95.

Elinson, R., del Pino, E. M., Townsend, D., Cuesta, F., and Eichhorn, P. 1990. A practical guide to the developmental biology of terrestrial-breeding frogs. *Biol. Bull. (Woods Hole)* 179: 163–177.

Franssen, R. A., Marks, S., Wake, D., and Shubin, N. 2005. Limb chondrogenesis of the seepage salamander, *Desmognathus aeneus* (Amphibia: Plethodontidae). *J. Morphol.* 265: 87–101.

Hall, B. K. 2005. *Bones and Cartilage: Developmental and Evolutionary Skeletal Biology*. Elsevier Academic Press, New York.

Hanken, J. 1986. Developmental evidence for amphibian origins. In M. K. Hecht, B. Wallace, and G. Prance (eds.). *Evolutionary Biology*. Plenum Press, New York, pp. 389–417.

Hanken, J. 2003. Direct Development. In B. Hall, W. Olson (eds.). *Keywords and concepts in Evolutionary Development Biology*. Harvard University Press, Cambridge, MA, pp. 97–102.

Hanken, J., et al. 2001. Limb development in a "nonmodel" vertebrate, the direct-developing frog *Eleutherodactylus coqui*. *J. Exp. Zool. (Mol. Dev. Evol.)* 291: 375–388.

Hinchliffe, J., and Griffiths, P. 1982. The prechondrogenic patterns in tetrapod limb development and their phylogenetic significance. In B. Goodwin, N. Holder, and C. Wylie (eds.). *Development and Evolution*. Cambridge University Press, Cambridge, UK, pp. 99–121.

Hinchliffe, J., and Johnson, D. 1980. *The Development of the Vertebrate Limb: An Approach Through Experiment, Genetics, and Evolution*. Clarendon Press, Oxford, UK.

Hinoi, E., et al. 2006. Runx2 inhibits chondrocyte proliferation and hypertrophy through its expression in the perichondrium. *Genes Dev.* 20: 2937–2942.

Holmgren, N. 1933. On the origin of the tetrapod limb. *Acta Zool.* 14: 184–295.

Joyce, S., and Cohen, A. 1970. The interphalangeal area of *Rana pipiens*: a light and electron microscopic study of the development of a fibrocartilaginous joint (symphysis). *J Morphol.* 130: 315–336.

Kerney, R., Gross, J. B., and Hanken, J. 2007a. Runx2 is essential for larval hyobranchial cartilage formation in *Xenopus laevis*. *Dev. Dyn.* 236: 1650–1662.

Kerney, R., Meegaskumbura, M., Manamendra-Arachchi, K., and Hanken, J. 2007b. Cranial ontogeny in *Philautus silus* (Anura: Ranidae: Rhacophorinae) reveals few similarities with other direct-developing anurans. *J. Morphol.* 268: 715–725.

Kim, I. S., Otto, F., Zabel, B., and Mundlos, S. 1999. Regulation of chondrocyte differentiation by Cbfa-1. *Mech. Dev.* 80: 159–170.

Komori, T., et al. 1997. Targeted disruption of *cbfa1* results in a complete lack of bone formation owing to a maturational arrest of osteoblasts. *Cell* 89: 7755–7764.

Linsenmayer, T. F., and Hendrix, M. J. 1980. Monoclonal antibodies to connective tissue macromolecules: type II collagen. *Biochem. Biophys. Res. Commun.* 92: 440–446.
Mahmood, R., et al. 1995. A role for FGF-8 in the initiation and maintenance of vertebrate limb bud outgrowth. *Curr. Biol.* 5: 797–806.
Mercader, N., Leonardo, E., Piedra, M., Martinez-A, C., Ros, M., and Torres, M. 2000. Opposing RA and FGF signals control proximodistal vertebrate limb development through regulation of Meis genes. *Development* 127: 3961–3970.
Nakamura, E., Nguyen, M. T., and Mackem, S. 2006. Kinetics of tamoxifen-regulated Cre activity in mice using a cartilage-specific CreER(T) to assay temporal activity windows along the proximodistal limb skeleton. *Dev. Dyn.* 235: 2603–2612.
Nieuwkoop, P. D., and Faber, J. 1994. *Normal table of Xenopus laevis (Daudin)*. Garland Publishing, New York, London.
Niswander, L., Tickle, C., Vogel, A., and Martin, G. 1994. Function of FGF-4 in limb development. *Mol. Reprod. Dev.* 39: 83–89.
Orton, G. 1951. Direct development in frogs. *Turtox News* 29: 2–6.
Otto, F., et al. 1997. Cbfa1, a candidate gene for cleidocranial dysplasia syndrome, is essential for osteoblast differentiation and bone development. *Cell* 89: 765–771.
Richardson, M. K., Carl, T., Hanken, J., Elinson, R., Cope, C., and Bagley, P. 1998. Limb development and evolution: a frog embryo with no apical ectodermal ridge. *J. Anat.* 192: 379–390.
Sampson, L. V. 1900. Unusual modes of breeding and development among anura. *Am. Nat.* 24: 687–715.
Saunders, J. W. Jr. 1948. The proximo-distal sequence of origin of the parts of the chick wing and the role of the ectoderm. *J. Exp. Zool.* 108: 363–403.
Shubin, N., and Wake, D. 2003. Morphological variation, development, and evolution of the limb skeleton of salamanders. In H. Heatwole and M. Davies (eds.). *Amphibian Biology. Vol. 5: Osteology*. Surrey Beatty and Sons, Chipping Norton, Australia, pp. 1782–1808.
Shubin, N. H., and Alberch, P. 1986. A morphogenetic approach to the origin and basic organization of the tetrapod limb. In M. K. Hecht, B. Wallace, and G. Prance (eds.). *Evolutionary Biology*. Plenum Press, New York, pp. 319–387.
Sive, H. L., Grainger, R. M., and Harland, R. M. 2000. *Early Development of Xenopus laevis*. Cold Spring Harbor Laboratory Press, Cold Spring Harbor, New York.
Summerbell, D., Lewis, J., and Wolpert, L. 1973. Positional information in chick limb morphogenesis. *Nature* 244: 492–496.
Sun, X., Mariani, F. V., and Martin, G. R. 2002. Functions of FGF signalling from the apical ectodermal ridge in limb development. *Nature* 418: 501–508.
Swalla, B. J., Upholt, W. B., and Solursh, M. 1988. Analysis of type II collagen RNA localization in chick wing buds by in situ hybridization. *Dev. Biol.* 125: 51–58.
Tabin, C., and Wolpert, L. 2007. Rethinking the proximodistal axis of the vertebrate limb in the molecular era. *Genes Dev.* 21: 1433–1442.
Tarin, D., and Sturdee, A. 1971. Early limb development in *Xenopus laevis*. *J. Embryol. Exp. Morphol.* 26: 169–179.
Tarin, D., and Sturdee, A. 1974. Ultrastructural features of ectodermal–mesenchymal relationships in the developing limb of *Xenopus laevis*. *J. Embryol. Exp. Morphol.* 31: 287–303.
Townsend, D., and Stewart, M. 1985. Direct development in *Eleutherodactylus coqui* (Anura: Leptodactylidae): a staging table. *Copeia* 1985: 423–436.
Trueb, L., and Hanken, J. 1992. Skeletal development in *Xenopus laevis* (Anura: Pipidae). *J. Morphol.* 214: 1–41.
Tschumi, P. 1957. The growth of the hindlimb bud of *Xenopus laevis* and its dependence upon the epidermis. *J. Anat.* 91: 149–173.
Wake, D., and Shubin, N. 1998. Limb development in the Pacific giant salamanders, *Dicamptodon* (Amphibia, Caudata, Dicamptodontidae). *Can. J. Zool.* 76: 2058–2066.
Welten, M., Verbeek, F., Meijer, A., and Richardson, M. K. 2005. Gene expression and digit homology in the chicken embryo wing. *Evo. Dev.* 7: 18–28.
Wright, E., et al. 1995. The Sry-related gene Sox9 is expressed during chondrogenesis in mouse embryos. *Nat. Genet.* 9: 15–20.

SUPPLEMENTARY MATERIALS

The following material for this article online is available:

Appendix S1. Online Supporting Material.

Fig. A1. Phylogenetic tree of representative SoxE class genes based on Clustal X amino acid alignment of 590 amino acids. Monophyly of Sox9 and Sox10 orthologs, with Sox8 as a sister group is consistent with previous Neighbor Joining (Zhang et al. 2006), parsimony, Bayesian, and likelihood analyses (Wada et al. 2006). The paraphyly of zebrafish sox9a and sox9b may be attributable to taxon sampling. This division was not found by Zhang et al. (2006), who included other teleost sox9 paralogs. McCauley and Bronner-Fraser (2006) did not use both zebrafish Sox9 paralogs in their analysis.

Fig. A2. Phylogenetic tree of representative fibrillar collagens based on a Clustal X alignment of 182 amino acids from the non-collagenous C-terminus domain. Monophyly of the col1a1, col2a1 and col3a1 clade is also found in previous minimum evolution analyses (Zhang, Miyamoto, and Cohn 2006). However, the analysis of Zhang et al. (2006) weakly supported the sister relationship of col3a1 and col1a1 clades (bootstrap support of 43), instead of the col1a1 - col2a1 sister relationship found here. The col1a1 – col2a1 sister relationship was found in a previous Bayesian analyses which also had differing placements of col1a2 and col5a1 (Zhang et al., 2006 — supporting online material). A separate maximum likelihood analysis describes the relationships of these three clades as a polytomy that includes col1a2 and col5a1 (Rennert et al. 2003).

Fig. A3. Phylogenetic tree of vertebrate runx family members based on a ClustalX alignment of the 132 amino acid DNA-binding runt domain. The sister relationship of runx2 and runx3, with runx1 as an outgroup, coincides with the maximum likelihood analysis of Rennert et al. (2003) and the Bayesian analysis of Pinto et al. (2005). It differs from the neighbor-joining tree of Levanon (2003) and maximum likelihood analysis of Pinto et al. (2005), both of which show a sister relationship of runx2 and runx1 with runx3 as an outgroup. This outgroup relationship of runx3 has been taken to indicate the ancestral runx role in neurogenesis of the reflex arc (Glusman et al. 2004), although this claim is not substantiated by experimental analysis of invertebrate runt genes. The neighbor-joining analysis of Glusman et al. (2004) reveals a basal polytomy of runx1 and runx3 in relation to the runx2 clade.

This material is available as part of the online article from: http://www.blackwell-synergy.com/doi/abs/10.1111/j.1525-142X.2008.00255.x (This link will take you to the article abstract).

Please note: Blackwell Publishing is not responsible for the content or functionality of any supplementary materials supplied by the authors. Any queries (other than missing material) should be directed to the corresponding author for the article.